Pham, T. and Hadi, M. and Youssef, J. 2015. Optimized FRP Wrapping Schemes for Circular Concrete Columns under Axial Compression. Journal of Composites for Construction. 19 (6).

Optimized FRP Wrapping Schemes for Circular Concrete Columns under Axial Compression

Thong M. Pham A.M.ASCE[1], Muhammad N.S. Hadi, F.ASCE[2] and Jim Youssef[3]

Abstract

This study investigates the behavior and failure modes of fiber-reinforced-polymer (FRP) confined concrete wrapped with different FRP schemes, including fully wrapped, partially wrapped and non-uniformly wrapped concrete cylinders. By using the same amount of FRP, this study proposes a new wrapping scheme that provides a higher compressive strength and strain for FRP-confined concrete, in comparison with conventional fully wrapping schemes. A total of thirty three specimens were cast and tested, with three of these specimens acting as reference specimens and the remaining specimens wrapped with different types of FRP (CFRP and GFRP) by different wrapping schemes. For specimens that belong to the descending branch type, the partially wrapped specimens had a lower compressive strength but a higher axial strain as compared to the corresponding fully wrapped specimens. In addition, the non-uniformly wrapped specimens achieved both a higher compressive strength and axial strain in comparison with the fully wrapped specimens. Furthermore, the partially wrapping scheme changes the failure modes of the specimens and the angle of the failure surface. A new equation that can be used to predict the axial strain of concrete cylinders wrapped partially with FRP is proposed.

CE Database subject headings: Fiber Reinforced Polymer; Confinement; Concrete columns; Strain; Stress-strain relation; Concrete; Cylinders.

[1]Postdoctoral Research Associate, School of Civil and Mechanical Engineering, Curtin University, Kent Street, Bentley, WA 6102, Australia; Formerly, PhD Scholar, School of Civil, Mining and Environmental Engineering, University of Wollongong, Wollongong, NSW 2522, Australia. Email: thong.pham@curtin.edu.au
[2]Associate Professor, School of Civil, Mining and Environmental Engineering, University of Wollongong, Wollongong, NSW 2522, Australia (corresponding author). Email: mhadi@uow.edu.au
[3]Ph.D. Candidate, School of Civil, Mining and Environmental Engineering, University of Wollongong, Wollongong, NSW 2522, Australia. Email: jy201@uowmail.edu.au

Introduction

Fiber Reinforced Polymer (FRP) has been commonly used to strengthen existing reinforced concrete (RC) columns in recent years. In such cases, FRP is a confining material for concrete in which the confinement effect leads to increase in the strength and ductility of columns. In early experimental studies that focused on retrofitting RC columns with FRP, the columns were usually wrapped fully with FRP sheets. This wrapping scheme provides continuous confinement to the columns along their longitudinal axes. Most of the studies in the literature focus only on columns fully wrapped with FRP (Chaallal et al. 2003; Hadi et al. 2013; Pham et al. 2013; Pham and Hadi 2014a; Smith et al. 2010). In addition, columns wrapped partially with FRP have also been proven to show increases in strength and ductility, as compared to equivalent unconfined columns (Colomb et al. 2008; Maaddawy 2009; Turgay et al. 2010). However, there is no study that makes a comparison of the confinement efficacy between partially and fully wrapping schemes in terms of optimization of the FRP amount. In addition, the progressive failure of those specimens has not been extensively studied. Therefore, it is necessary to investigate the confinement efficacy and failure mechanisms of columns partially wrapped versus columns fully wrapped with FRP.

In addition, the available design guidelines for columns wrapped with FRP (ACI 440.2R-08 2008; *fib* 2001; TR 55 2012) are utilized to estimate the capacities of partially FRP-wrapped specimens. Among these studies, ACI-440.2R (2008) and technical report TR 55 (2012) do not provide information about the confinement effect of concrete columns partially wrapped with FRP. Meanwhile, *fib* (2001) suggests a reduction factor to take into account the effect of partial wrapping columns. The study by *fib* (2001) adopts an assumption proposed by Mander et al. (1988) for the confinement effect of steel ties in RC columns to analyze the efficacy of FRP partially wrapped columns. Therefore, there has been a lack of theoretical and experimental works about partial FRP-confined concrete. For this reason, an experimental program was developed in this study to compare the confinement efficacy of FRP partially wrapped columns as compared to FRP fully wrapped columns. The same amount of FRP was wrapped onto identical concrete columns by different wrapping schemes to achieve an optimized wrapping design.

Confinement Mechanism

Fully Wrapped Columns

In the literature, the term "FRP confined concrete" is understood automatically as concrete wrapped fully with FRP. When a circular concrete column is horizontally wrapped with FRP around its perimeter, the whole column is confined by the lateral pressure exerted from the FRP jackets as shown in Fig. 1a. Many studies have been carried out to investigate the behaviors and estimate the capacities of columns wrapped fully with FRP (De Luca and Nanni 2011; Lam and Teng 2003; Pham and Hadi 2014b; Pham and Hadi 2014c; Teng et al. 2009; Toutanji 1999; Wu and Zhou 2010). The confining pressure is assumed to be uniform in the cross section and along the axial axis of the circular columns. Among the existing studies, the model proposed by Lam and Teng (2003) is adopted in this study to calculate the compressive strength for columns wrapped fully with FRP as follows:

$$\frac{f_{cc}^{'}}{f_{co}^{'}} = 1 + 3.3\frac{f_l}{f_{co}^{'}} \qquad (1)$$

where $f_{cc}{}'$ and $f_{co}{}'$ are respectively the compressive strength of confined concrete and unconfined concrete, and f_l is the effective confining pressure as follows:

$$f_l = \frac{2E_f \varepsilon_{fe} t}{D} \qquad (2)$$

where E_f is the elastic modulus of FRP, t is the nominal thickness of FRP jacket, D is the diameter of the column section, and ε_{fe} is the actual rupture strain of FRP in the hoop direction. The model by Lam and Teng (2003) is chosen because it provides a reasonable accuracy with a very simple form. The simplicity of the model by Lam and Teng (2003) is utilized to establish a new and simple strain model, which is presented in the sections below. The strain model proposed by Pham and Hadi (2013) is adopted to calculate the compressive axial strain of confined concrete as follows:

$$\varepsilon_{cc} = \varepsilon_{co} + \frac{2ktf_{fe}\varepsilon_{fe}}{Df'_{co} + 3.3tf_{fe}} \qquad (3)$$

where ε_{cc} is the ultimate axial strain of confined concrete, ε_{co} is the axial strain at the peak stress of unconfined concrete, k = 7.6 is the proportion factor, and f_{fe} is the actual rupture strength of FRP.

Partially Wrapped Columns

As mentioned above, concrete columns wrapped partially with FRP have been experimentally verified to increase their strength and ductility. Concrete columns partially wrapped with FRP are less efficient in nature than fully wrapped columns as both confined and unconfined zones exist (Fig. 1b). An approach similar to the one proposed by Sheikh and Uzumeri (1980) is adopted to determine the effective confining pressure on the concrete core. The effective confining pressure is assumed to be exerted effectively on the part of the concrete core where the confining pressure has fully developed due to the arching action as shown in Fig. 1b. The arching effect is assumed to be described by a second-degree parabola with initial slope of 45^0. In such a case, a confinement effective coefficient (k_e) is introduced to take the partial wrapping into account as follows:

$$k_e = \frac{A_e}{A_c} = \left(1 - \frac{s}{2D}\right)^2 \quad (4)$$

where A_e and A_c are respectively the area of effectively confined concrete core and the cross-sectional area, and s is the clear spacing between two FRP bands. Consequently, the compressive strength of concrete columns wrapped partially with FRP could be calculated as:

$$\frac{f'_{cc}}{f'_{co}} = 1 + 3.3k_e \frac{f'_l}{f'_{co}} \quad (5)$$

Where k_e is estimated based on Eq. 4 and f_l' shown in the following equation is the equivalent confining pressure from the FRP, assumed to be uniformly distributed along the longitudinal axis of the column.

$$f'_l = \frac{2E_f \varepsilon_{fe} t}{D} \frac{w}{w+s} \quad (6)$$

where w is the width of FRP bands and s is the clear spacing between FRP bands as shown in Fig. 1b.

Experimental Program

Design of Experiments

A total of thirty three FRP confined concrete cylinders were cast and tested at the High Bay Laboratory of the University of Wollongong. The dimensions of the concrete cylinder specimens were 150 mm in diameter and 300 mm in height. All the specimens were cast from the same batch of concrete. The 28 day cylinder compressive strength was 52 MPa.

The experimental program was composed of several groups of cylinders in order to evaluate the confinement efficacy between partially and fully wrapping schemes in terms of optimization of the wrapping schemes. The notation of the specimens consists of three parts: the first part states the type of confining FRP material, with “G” and “C” representing GFRP and CFRP respectively. The second part is either a letter “R”, “F”, and “P” stating the name of the sub-group, namely, reference group (R), fully wrapped group (F) and partially wrapped group (P). The last part of the specimen notation is a number which indicates the number of FRP layers. Details of the specimens are presented in Table 1.

The partially wrapped specimens contain FRP bands which are 25 mm in width spaced evenly along the height of the specimen. The optimized partially wrapped specimens include two numbers in the notation, for example GP31. The first number indicates the number of 25 mm evenly spaced partial FRP layers and the second number depicts the number of FRP layers in between these evenly spaced partial layers. These specimens were designed such that they follow a non-uniform wrapping configuration but ensure the specimen is fully confined at every location. The thicker band is called a tie band and the thinner band is called a cover band. Taking specimen GP31 as an example, the tie bands have three FRP layers which are 25 mm in width, while the cover bands have one FRP layer as shown in Figure 2. Three identical specimens were made for each wrapping scheme.

In order to analyze the confinement effectiveness between different wrapping schemes, the specimens were divided in four groups (as shown in Table 1) such that the specimens in each group incorporate the same amount of FRP but in a different wrapping scheme, either fully, partially or optimized non-uniformly wrapped. The specimens in the first group are reference specimens which did not include any internal or external reinforcement. The specimens in the second and third groups were confined by GFRP and CFRP respectively, such that the fully, partially and optimized non-uniform wrapping schemes were equivalent to two layers of full wrapping. Similarly, the wrapping schemes of the specimens in the fourth group were equivalent to three layers of full wrapping.

After 28 days, the specimens were wrapped with a number of FRP layers as shown in Table 1. The adhesive used was a mixture of epoxy resin and hardener at 5:1 ratio. Before the first layer of FRP was attached, the adhesive was spread onto the surface of the specimen and CFRP was attached onto the surface with the main fibers oriented in the hoop direction. After the first layer, the adhesive was spread onto the surface of the first layer of FRP and the second layer was continuously bonded. The third layer of FRP was applied in a similar manner, ensuring that 100 mm overlap was maintained. The ends of each wrapped specimen were strengthened with additional one layer of FRP strips 25 mm in width.

Instrumentation

In order to measure the hoop strains of the FRP jacket, three strain gages with a gage length of 5 mm were attached at the mid height of the specimens and evenly distributed away from the overlap for the fully wrapped specimens. In the partially wrapped specimens, three strain gages were bonded symmetrically on a tie band and other three were bonded on a cover band at midheight of the specimen.

Furthermore, a longitudinal compressometer as shown in Fig. 3 was used to measure the axial strain of the specimens. A Linear variable differential transformer (LVDT) was mounted on the upper ring and the tip of the LVDT rests on an anvil. The readability, the accuracy, and the repeatability of the LVDT complies with the Australian standard (Australian Standard-1545 1976).

The compression tests for all the specimens were conducted using the Denison 5000 kN capacity testing machine. The specimens were capped with high strength plaster to ensure full contact between the loading plate and the specimen. Calibration was carried out to ensure that the specimens were placed at the center of the testing machine. Each specimen was first loaded to around 30% of its unconfined capacity to check the alignment. If required, the specimen was unloaded, realigned, and loaded again. The tests were conducted as deflection controlled with a rate of 0.5 mm/min. The readings of the load, LVDT and strain gages were taken using a data logging system and were subsequently saved in a control computer.

Experimental Results

Preliminary tests

The actual compressive strength of unconfined concrete calculated from three reference specimens (R1, R2, and R3) was 54 MPa. The axial strain of unconfined concrete at the maximum load was 0.23 %. In this study two types of CFRP were used to confine the concrete, which both had a unidirectional fiber density of 340 g/m^2 and a nominal thickness of 0.45 mm, but with varying nominal widths of 75 mm and 25 mm. The GFRP utilized had a unidirectional fiber density of 440 g/m^2, a nominal thickness of 0.35 mm and a nominal width of 50 mm.

Five coupons for each type of FRP were made according to ASTM D7565 (2010) and tested to determine the mechanical properties. The two types of CFRP coupons were made of three layers of FRP with a nominal thickness of 1.35 mm and both types had very similar properties as shown in Table 2. For simplicity the coupons produced from the 75 mm tape are denoted by CFRP (75) while the coupons from the 25 mm tape are referred to as CFRP (25). For GFRP, two-layered coupons containing two overlapping fiber sheets were prepared and tested. The nominal thickness of the coupons was 0.7 mm. All coupons had the dimensions 25 mm x 250 mm. The epoxy resin had 54 MPa tensile strength, 2.8 GPa tensile modulus and 3.4% tensile elongation (West System n.d. 2015).

Failure Modes

All specimens were tested until failure. The specimens wrapped fully with FRP (CF2, CF3, and GF2) failed by rupture of FRP at the midheight. The failure surface of the fully wrapped specimens was found to be approximately 45 degree inclined, as shown in Fig. 4a. Meanwhile, the partially wrapped specimens (CP40, CP60, and GP40) showed many small cracks on the concrete surface at a stress equal to the unconfined concrete strength, as shown in Fig. 4b. The concrete between the FRP bands, close to the outer surface of the specimen, started crushing while the concrete core was still confined by the FRP. Cracks on the concrete surface developed as the applied load increased, as shown in Fig. 4c. At the very high stress level, the concrete between the FRP bands spalled off while the concrete under the FRP bands and the core were still confined. These specimens then failed explosively by FRP rupture at the midheight (Fig. 4d).

The angle of the failure surface with respect to the horizon for the partially wrapped specimens was significantly different from the fully wrapping specimens. As shown in Fig. 4d, the failure surface took place at the spacing between FRP bands. This change of the failure surface depends on the wrapping schemes and the stiffness of the FRP bands. When the axial stress of the confined concrete was higher than the unconfined concrete strength, the 45 degree failure surface may have originally transpired in the concrete cores, but cracks were arrested by FRP bands under the high stress stage. If the stiffness of the FRP bands is not strong enough (Specimen GP40) to prevent the development of the cracks, the failure surface takes place at approximately 45 degrees as shown in Fig. 4e. In contrast, the stiffness of the FRP bands in Specimens CP40 and CP60 is great enough so that it changed the failure surface as depicted in Fig. 4d. It is worth mentioning that the stiffness of the FRP bands affects the tangent modulus of FRP-confined concrete. Tamuzs et al. (2008) suggested that the low value of the tangent modulus causes column stability collapse directly as the unconfined concrete strength level is surpassed.

Furthermore, specimens with optimized non-uniform wrapping schemes showed a different failure mode as compared to the others. At a stress level equal to the unconfined concrete strength, the concrete was still confined by the FRP tie bands and cover bands. During the loading process, the lateral strains of the tie bands and the cover bands were almost identical, with the exception of Specimen CP40_3. The failure modes of these specimens are similar to those of the full wrapping specimens. The Non-uniform wrapped specimens failed by FRP rupture simultaneously at the two bands (tie band and cover band) at the midheight, as shown in Fig. 4f. It is worth mentioning that intermittent confinement resulted from partial confinement (Specimens GP40, CP40, and CP60) makes the concrete to communicate directly with the surroundings, for instance moisture, heat, and evaporation.

Stress-Strain Relation

Stress-strain relations of the tested specimens were divided into two main types based on the shape of the stress-strain curves. These included specimens in the ascending branch type and descending branch type. A FRP confined concrete column exhibits the ascending type curve as a significant improvement of the compressive strength and strain of a FRP confined concrete column could be expected. Otherwise, FRP confined concrete with a stress-strain curve of the descending type illustrates a concrete stress at the ultimate strain below the compressive strength of unconfined concrete. Specimens wrapped with glass fiber are designed to behave as the descending branch type while specimens wrapped with carbon fiber belong to the ascending branch type. Details of all tested specimens are summarized in Table 3.

Stress-strain relations of specimens wrapped by equivalent two GFRP layers were plotted in Fig. 5. The specimens which were wrapped with an equivalent of two layers of FRP had identical stress-strain curves at the early stages of loading and experienced slight differences at the latter stage of testing. Specimens GF2 and GP40 had the descending branch type stress-strain curve while the stress-strain curves of Specimens GP31 kept constant after reaching the unconfined concrete strength and then increased again to failure. The axial stress of Specimens GF2 reached the unconfined concrete strength (54 MPa) and then kept constant until the FRP failed by rupture as shown in Fig. 5a. The average compressive confined concrete strength and strain of Specimens GF2 are 57 MPa and 0.97 %, respectively. Although Specimens GP40 obtained a lower maximum stress (53 MPa) as compared to that of Specimens GF2, they achieved a larger maximum axial strain (1.18%) than the former specimens. The axial strain of Specimens GP40 increased by 21.31 % as compared to that of Specimens GF2 (Fig. 5b). Meanwhile, Specimens GF31 achieved both a higher maximum axial stress (60 MPa) and axial strain (1.02 %), as compared to Specimen GF2, as shown in Fig. 5c.

Apart from the specimens above, the specimens which were wrapped with an equivalent of two layers of FRP, had similar stiffness during the whole loading process, as shown in Fig. 6. The maximum axial stress of Specimens CF2 was 99 MPa and its corresponding axial strain was 2.13%. Specimens CP40 reached the maximum axial stress at 95 MPa and the corresponding axial strain at 2.08%. Specimen CP40_1 failed by premature rupture of FRP (ε_l = 1.18 %) that resulted in very lower maximum axial stress. The average maximum axial stress and axial strain of Specimens CP31 were 98 MPa and 2.12 %, respectively.

The specimens that were wrapped with an equivalent of three layers of FRP had similar stress-strain curves but experienced a slight difference in the axial stiffness for the whole loading process as shown in Fig. 7. Specimens CF3 obtained average maximum axial stress and strain at 122 MPa and 2.84 %, respectively (Fig. 7a). The partially wrapped Specimens CP60 again had a lower compressive strength but higher axial strain as compared to those of

Specimens CF3. As shown in Fig. 7b, Specimens CP60 failed at the average compressive strength of 116 MPa and axial strain of 3.25 %. The axial strain for the specimens CP60 increased by 14.33% in comparison with the Specimens CF3. As compared to Specimens CF3, the non-uniformly wrapped Specimens CP42 had both higher compressive strength and axial strain. Fig. 7d shows that Specimens CP42 failed at the average compressive strength of 128 MPa and strain of 3.16 %. As a result, the compressive strength and axial strain of these specimens respectively increased by 5.29 % and 11.16 % as compared to Specimens CF3. In order to compare the effectiveness of different wrapping schemes, the stress-strain curves of five specimens are plotted in Fig. 7e. In reference to this figure, it can be seen that the partially wrapped Specimens CP60 experienced a lower maximum stress and a higher maximum strain, as compared to Specimens CF3. On the hand, the non-uniformly wrapped specimens CP42 experienced both a higher maximum strain and stress in comparison with Specimens CF3. These findings have also been confirmed by specimens in Group GF2, as shown in Fig. 5d.

Analysis and Discussions

Lateral Strain

The lateral strain of all the specimens are obtained by taking the average of readings from three strain gages evenly placed along the FRP at locations away from the overlap. For each specimen, the actual rupture strain of FRP is presented in Table 3. In order to investigate the effectiveness of the fiber, the strain efficiency factor k_ε is adopted, which is the ratio of the actual rupture strain of FRP in confined specimens and the rupture strain of the FRP obtained from the tensile coupon testing. As can be seen from Table 3, the strain efficiency factors of fully wrapped specimens are approximately 0.83 and 0.87 for glass fiber and carbon fiber, respectively. For glass fiber, the strain efficiency factor of partially wrapped specimens was

0.77 and the corresponding number for non-uniformly wrapped specimens was 0.91. Meanwhile, the strain efficiency factor of specimens partially wrapped with CFRP was 0.80 and the corresponding number for non-uniformly wrapped specimens was 0.91. The experimental results have shown that the effectiveness of the fiber reduces in the partial wrapping scheme, but increases in the non-uniformly wrapping scheme.

There is a consensus that the presence of the triaxial stress state in FRP affects the actual rupture strain of the fiber (Chen et al. 2013). In this experimental program, it is obvious that the axial stress of the FRP jackets in the fully wrapped specimens is higher than that of the non-uniformly wrapped specimens. The discontinuity of the jacket in the non-uniformly wrapped specimens reduces the axial stress of the FRP jacket, which could be a reason for the increase in the strain efficiency factor in these specimens. Thus, the non-uniformly wrapped specimens had a higher value of k_{ε}, resulting in a higher confined strength and strain. In other words, the discontinuity of the jackets of the partially wrapped specimens did not increase the strain efficiency factor. The partially wrapped specimens experienced a different failure mode as compared with the other wrapping schemes. This different failure mode in partially wrapped specimens may be the reason behind the slight decrease in the strain efficiency factor for these specimens.

In addition, the lateral strain of the non-uniformly wrapped specimens at both the tie bands and cover bands of the FRP is investigated. For example, the lateral strain – axial stress of Specimen CP40_3 (Fig. 8), illustrates that the lateral strain of FRP in a cover band is slightly higher than that of a tie band at any axial stress state. However, there was no difference in the lateral strain in other specimens.

Analytical Verification

In order to predict the compressive strength of the tested specimens, the procedure in the section Confinement Mechanism is used. It is noted that the actual lateral strain of each specimen was used in these calculations. The maximum axial strain of the tested specimens is predicted based on the study by Pham and Hadi (2013), in which the relationship between the energies absorbed by the whole column and the FRP was taken into account. Pham and Hadi (2013) assumed that the additional energy in the column core equals the area under the experimental stress-strain curves starting from the value of unconfined concrete strain:

$$U_{cc} = \int_{\varepsilon_{co}}^{\varepsilon_{cc}} f_c d\varepsilon_c = \frac{(\varepsilon_{cc} - \varepsilon_{co})(f'_{co} + f'_{cc})}{2} \quad (7)$$

where U_{cc} is the volumetric strain energy of confined concrete, f_c is the stress of confined concrete, and $d\varepsilon_c$ is an increment of the axial strain.

However, the concrete in the partially wrapped columns is confined in the effective area as shown in Fig. 1. To determine the volumetric strain energy of confined concrete for the whole columns, the value of the confined concrete strength needs to be modified by the confinement effective coefficient (k_e), which leads to the following equation:

$$U_{cc} = \int_{\varepsilon_{co}}^{\varepsilon_{cc}} f_c d\varepsilon_c = \frac{(\varepsilon_{cc} - \varepsilon_{co})(f'_{co} + k_e f'_{cc})}{2} \quad (8)$$

Similarly, the energy absorbed by FRP could be calculated as follows:

$$W_f = \rho_f A_c (\frac{1}{2} f_{fe} \varepsilon_{fe}) \quad (9)$$

where W_f is the strain energy of FRP, and ρ_f is the volumetric ratio of FRP as shown in Eq. 10.

$$\rho_f = \frac{4t}{D} \tag{10}$$

The compressive strain of columns partially wrapped with FRP is calculated as follows**:**

$$\varepsilon_{cc} = \varepsilon_{co} + \frac{2ktf_{fe}\varepsilon_{fe}}{D\left(f_{co}^{'} + k_e f_{cc}^{'}\right)} \tag{11}$$

The predicted results of the compressive strength and strain of the tested specimens are presented in Table 4. This table has shown that the predicted results are quite close to the experimental results.

Conclusions

This study presented an experimental study on the optimization of concrete cylinders wrapped with FRP. The same amount of FRP was used in each group of specimens but with different wrapping schemes, in order to investigate the confinement efficacy between fully, partially and a proposed non-uniform wrapping scheme for FRP-confined concrete. The findings presented in this study are summarized as follows:

1. For specimens belonging to the descending branch type, the partially wrapped specimens had a lower compressive strength but a higher strain as compared to the corresponding fully wrapped specimens. On the other hand, the non-uniform wrapped specimens experienced both a higher compressive strength and axial strain in comparison with the fully wrapped specimens.

2. For heavily FRP-confined specimens (CF3, CP60, CP51 and CP42), partial and non-uniform wrapped specimens provided a higher axial strain as compared to that of fully wrapped specimens.

3. The partial wrapping scheme changes the failure modes of the specimens. If the FRP jackets are strong enough, the angle of the failure surface significantly reduces.

4. The actual rupture strain of the FRP jackets is different for each wrapping scheme. The strain efficiency factor in the full wrapping scheme is greater than that of the partial wrapping scheme but is less than that of the non-uniform wrapping scheme.

5. An equation is proposed to estimate the axial strain of partially FRP-confined concrete circular columns.

Finally, this study proposed a new wrapping scheme that uses the same amount of FRP as compared to the conventional fully wrapping scheme, in order to yield a higher compressive strength and strain. However, further studies are required to theoretically investigate the behavior of non-uniform wrapped specimens.

Acknowledgement

The authors would like to acknowledge the technical assistance of Messrs. Alan Grant, Cameron Neilson, Fernando Escribano, Ritchie McLean and Colin Devenish. The contribution of Mr. Elliot Davison is greatly appreciated. Furthermore, the first author would like to thank the Vietnamese Government and the University of Wollongong for the support of his full Ph.D. scholarship.

Notations

A_c = cross-sectional area;
A_e = area of effectively confined concrete core;
D = diameter of the column section;
$d\varepsilon_c$ = increment of the axial strain;
E_f = elastic modulus of FRP;

f_c = stress of concrete;

f_{fe} = actual rupture strength of FRP;

f_{cc}' = confined concrete strength;

f_{co}' = unconfined concrete strength;

f_l = effective confining pressure of a column;

f_l' = equivalent confining pressure from the FRP;

k = proportion factor;

k_e = confinement effective coefficient;

s = clear spacing between two FRP bands;

t = nominal thickness of FRP;

U_{cc} = volumetric strain energy of confined concrete;

W_f = strain energy of FRP;

w = width of FRP bands;

ε_{fe} = actual rupture strain of FRP in hoop direction;

ε_{cc} = ultimate axial strain of confined concrete;

ε_{co} = axial strain of the unconfined concrete at the maximum stress; and

ρ_f = volumetric ratio of FRP.

References

ACI 440.2R-08 (2008). "Guide for the Design and Construction of Externally Bonded FRP Systems for Strengthening Concrete Structures." *440.2R-08*, American Concrete Institute, Farmington Hills, MI.

ASTM (2010). "Standard test method for tensile properties of fiber reinforced polymer matrix composites used for strengthening of civil structures." *D7565:2010*West Conshohocken, PA.

Australian Standard-1545 (1976). "Methods for the Calibration and Grading of Extenometers." *1545-1976*Homebush, NSW 2140.

Chaallal, O., Shahawy, M., and Hassan, M. (2003). "Performance of axially loaded short rectangular columns strengthened with carbon fiber-reinforced polymer wrapping." *J Compos Constr*, 7(3), 200-208.

Chen, J., Li, S., and Bisby, L. (2013). "Factors Affecting the Ultimate Condition of FRP-Wrapped Concrete Columns." *J Compos Constr*, 17(1), 67-78.

Colomb, F., Tobbi, H., Ferrier, E., and Hamelin, P. (2008). "Seismic retrofit of reinforced concrete short columns by CFRP materials." *Compos Struct*, 82(4), 475-487.

De Luca, A., and Nanni, A. (2011). "Single-Parameter Methodology for the Prediction of the Stress-Strain Behavior of FRP-Confined RC Square Columns." *J Compos Constr*, 15(3), 384-392.

fib (2001). "Externally bonded FRP reinforcement for RC structures." *Bulletin*, 14, 138.

Hadi, M. N. S., Pham, T. M., and Lei, X. (2013). "New Method of Strengthening Reinforced Concrete Square Columns by Circularizing and Wrapping with Fiber-Reinforced Polymer or Steel Straps." *J Compos Constr*, 17(2), 229-238.

Lam, L., and Teng, J. G. (2003). "Design-oriented stress-strain model for FRP-confined concrete." *Constr Build Mater*, 17(6-7), 471-489.

Maaddawy, T. E. (2009). "Strengthening of Eccentrically Loaded Reinforced Concrete Columns with Fiber-Reinforced Polymer Wrapping System: Experimental Investigation and Analytical Modeling." *J Compos Constr*, 13(1), 13-24.

Mander, J. B., Park, R., and Priestley, M. J. N. (1988). "Theoretical Stress-Strain Model for Confined Concrete." *J Struct Eng*, 114(8), 1804-1826.

Pham, T. M., Doan, L. V., and Hadi, M. N. S. (2013). "Strengthening square reinforced concrete columns by circularisation and FRP confinement." *Constr Build Mater*, 49(0), 490-499.

Pham, T. M., and Hadi, M. N. S. (2013). "Strain Estimation of CFRP Confined Concrete Columns Using Energy Approach." *J Compos Constr*, 17(6), 04013001.

Pham, T. M., and Hadi, M. N. S. (2014a). "Confinement Model for FRP Confined Normal- and High-Strength Concrete Circular Columns." *Constr Build Mater*, 69, 83-90.

Pham, T. M., and Hadi, M. N. S. (2014b). "Predicting Stress and Strain of FRP Confined Rectangular/Square Columns Using Artificial Neural Networks." *J Compos Constr*, 18(6), 04014019.

Pham, T. M., and Hadi, M. N. S. (2014c). "Stress Prediction Model for FRP Confined Rectangular Concrete Columns with Rounded Corners." *J Compos Constr*, 18(1), 04013019.

Sheikh, S. A., and Uzumeri, S. M. (1980). "Strength and ductility of tied concrete columns." *Journal of the structural division*, 106(5), 1079-1102.

Smith, S. T., Kim, S. J., and Zhang, H. W. (2010). "Behavior and Effectiveness of FRP Wrap in the Confinement of Large Concrete Cylinders." *J Compos Constr*, 14(5), 573-582.

Tamužs, V., Tepfers, R., Zīle, E., and Valdmanis, V. "Mechanical behaviour of FRP-confined concrete columns under axial compressive loading." *Proc., 5th International engineering and construction conference (IECC'5). American Society of Civil Engineers, International Committee, Los Angeles Section*, 223-241.

Teng, J. G., Jiang, T., Lam, L., and Luo, Y. Z. (2009). "Refinement of a Design-Oriented Stress-Strain Model for FRP-Confined Concrete." *J Compos Constr*, 13(4), 269-278.

Toutanji, H. A. (1999). "Stress-strain characteristics of concrete columns externally confined with advanced fiber composite sheets." *ACI Mater J*, 96(3), 397-404.

TR 55 (2012). *Design guidance for strengthening concrete structures using fibre composite materials*, Concrete Society, Camberley.

Turgay, T., Polat, Z., Koksal, H. O., Doran, B., and Karakoç, C. (2010). "Compressive behavior of large-scale square reinforced concrete columns confined with carbon fiber reinforced polymer jackets." *Materials & Design*, 31(1), 357-364.

West System n.d. (2015). "Epoxy resins and hardeners - Physical properties." <http://www.westsystem.com/ss/typical-physical-properties>. (Jan. 31, 2015).

Wu, Y. F., and Zhou, Y. W. (2010). "Unified Strength Model Based on Hoek-Brown Failure Criterion for Circular and Square Concrete Columns Confined by FRP." *J Compos Constr*, 14(2), 175-184.

List of Figures

Figure 1. Confinement mechanism

Figure 2. Different wrapping schemes

Figure 3. Compressometer

Figure 4. Failure modes of the tested specimens

Figure 5. Stress-strain relation of Group GF2

Figure 6. Stress-strain relation of Group CF2

Figure 7. Stress-strain relation of Group CF3

Figure 8. Lateral strain – axial stress relationship of Specimen CP40_3

List of Table

Table 1. Test matrix

Table 2. Results of tensile tests on FRP flat coupon tests

Table 3. Experimental results of tested specimens

Table 4. Verification of the experimental results

Table 1. Test matrix

Group	No. of specimens	Type of FRP	Equivalent FRP layers with full wrapping	Width of each FRP band (w, mm)	Clear spacing (s, mm)	Type of Wrapping
R	3	-	-	-	-	
GF2	3			50	0	Full
GP40	3	GFRP	2	25	25	Partial
GP31	3			25	0	Non-uniform
CF2	3			75	0	Full
CP40	3	CFRP	2	25	25	Partial
CP31	3			25	0	Non-uniform
CF3	3			75	0	Full
CP60	3			25	25	Partial
CP51	3	CFRP	3	25	0	Non-uniform
CP42	3			25	0	Non-uniform

Table 2. Results of tensile tests on FRP flat coupons

Type of coupon specimen	Number of FRP layers	Width (mm)	Nominal thickness (mm)	Average Elastic Modulus (MN/mm)	Average Tensile Strength (kN/mm)	Average Ultimate Strain (mm/mm)
CFRP (75)[*]	3	25	1.35	133	2171	0.0163
CFRP (25)[**]	3	25	1.35	133	2157	0.0162
GFRP	2	25	0.70	29.5	582	0.0197

[*] CFRP (75) denotes the coupons made of the FRP sheets that have 75 mm width

[**] CFRP (25) denotes the coupons made of the FRP sheets that have 25 mm width

Table 3. Experimental results of tested specimens

Specimen	Maximum axial stress			Maximum axial strain			Maximum lateral strain		Strain efficiency factor
	f_{cc}' (MPa)	Average (MPa)	Increase# (%)	ε_{cc} (%)	Average (%)	Increase# (%)	ε_l (%)	Average (%)	k_ε
GF2_1	57			1.30			1.70		
GF2_2	56	57	-	0.63	0.97	-	1.31	1.64	0.83
GF2_3	57			0.98			1.91		
GP40_1	55			1.25			1.59		
GP40_2	53	53	-6.04	1.26	1.18	21.31	1.61	1.51	0.77
GP40_3	51			1.02			1.34		
GP31_1	62			1.31			1.87		
GP31_2	61	60	6.56	0.66	1.02	5.49	1.79	1.80	0.91
GP31_3	59			1.10			1.74		
CF2_1	97			1.87			1.35		
CF2_2	99	99	-	2.23	2.13	-	1.41	1.41	0.87
CF2_3	101			2.28			1.47		
CP40_1	86			1.58			1.18*		
CP40_2	95	95	-3.62	2.05	2.08	-2.02	-	1.30	0.80
CP40_3	96			2.12			1.42		
CP31_1	97			2.23			1.52		
CP31_2	97	98	-1.56	1.97	2.12	-0.32	1.52	1.52	0.94
CP31_3	99			2.16			1.50		
CF3_1	126			2.88			1.35		
CF3_2	118	122	-	2.58	2.84	-	1.37	1.39	0.86
CF3_3	122			3.06			1.45		
CP60_1	113			3.20			1.21		
CP60_2	118	116	-4.72	3.25	3.25	14.33	1.29	1.30	0.80
CP60_3	117			3.29			1.39		
CP51_1	117			2.96			1.34		
CP51_2	121	119	-2.04	3.21	3.09	8.58	1.52	1.43	0.88
CP51_3	108			2.17			1.16*		
CP42_1	124			3.12			1.53		
CP42_2	128	128	5.29	3.33	3.16	11.16	1.46	1.50	0.92
CP42_3	132			3.03			1.50		

* Specimens performed premature damage

Increase of a specimen compared to the fully wrapping specimens in the same group.

Table 4. Verification of the experimental results

Specimen	D (mm)	t (mm)	s (mm)	w (mm)	k_ε	f_l (MPa)	k_e (*)	Theoretical f_{cc} (**) (MPa)	Theoretical ε_{cc} (%)	Experimental f_{cc} (MPa)	Experimental ε_{cc} (%)	Δf_{cc} (%)	$\Delta\varepsilon_{cc}$ (%)
CF2	150	0.9	0	0	0.87	17	1.00	109	2.43	99	2.13	10	14
CP40	150	1.8	25	25	0.80	15	0.84	97	2.49	95	2.08	2	20
CF3	150	1.35	0	0	0.86	25	1.00	135	2.98	122	2.84	11	5
CP60	150	2.7	25	25	0.80	23	0.84	118	3.20	116	3.25	2	-2

Δf_{cc} and $\Delta\varepsilon_{cc}$ = difference between the theoretical values and the corresponding experimental values

(*) the values of k_e were calculated based on Equation 4

(**) the values of f_{cc} were calculated based on Equation 5

Fig. 1

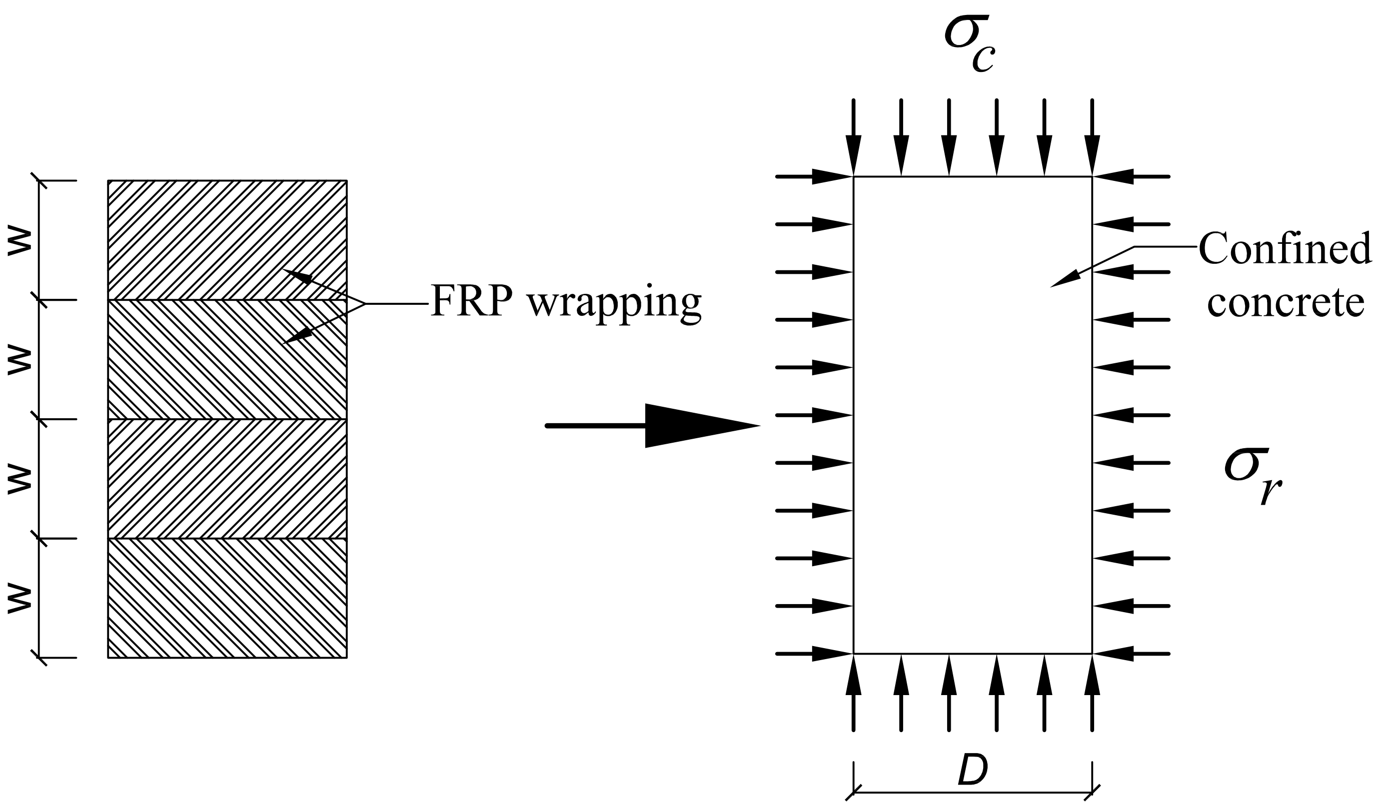

a) Concrete columns wrapped fully with FRP

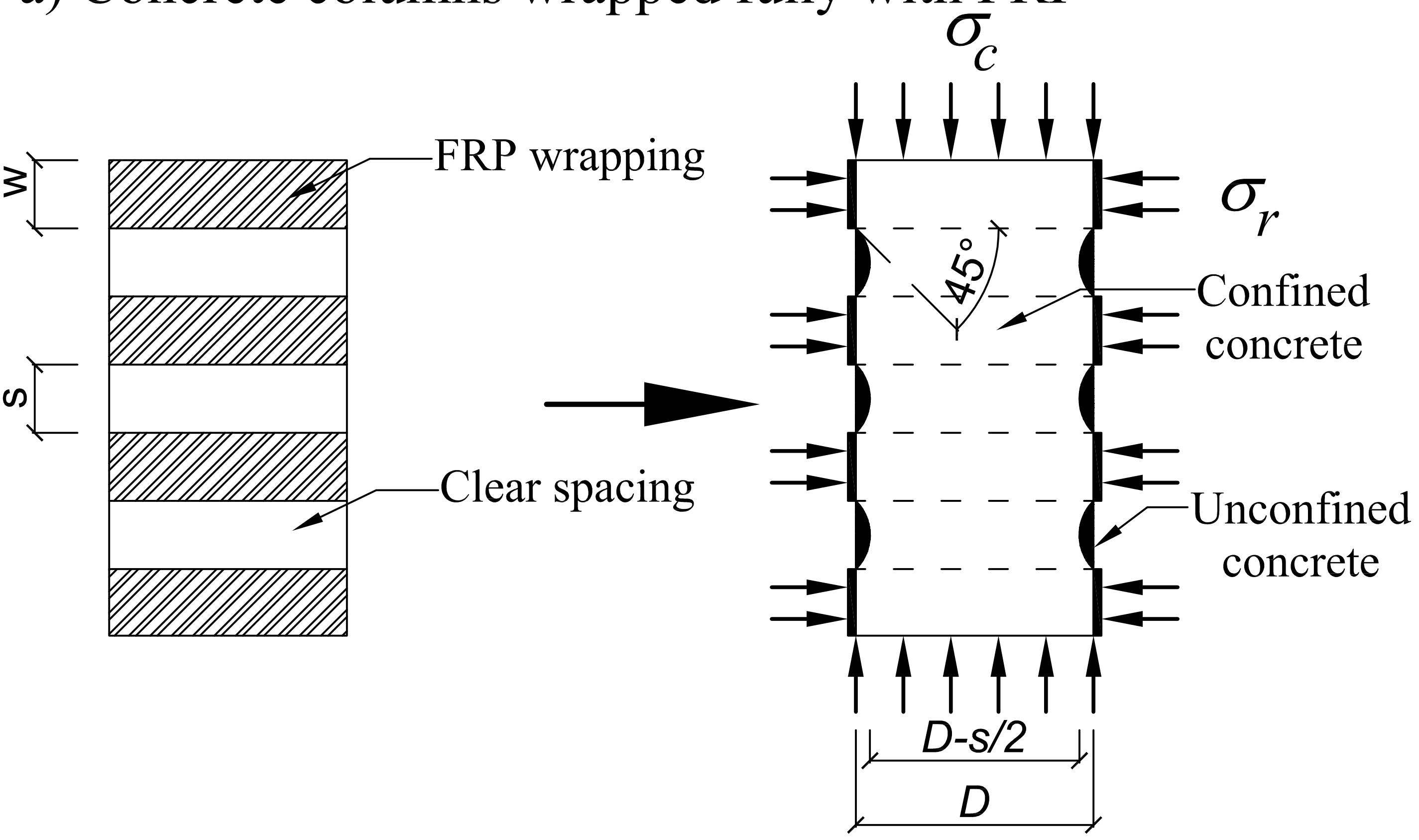

b) Concrete columns wrapped partially with FRP

Fig. 2

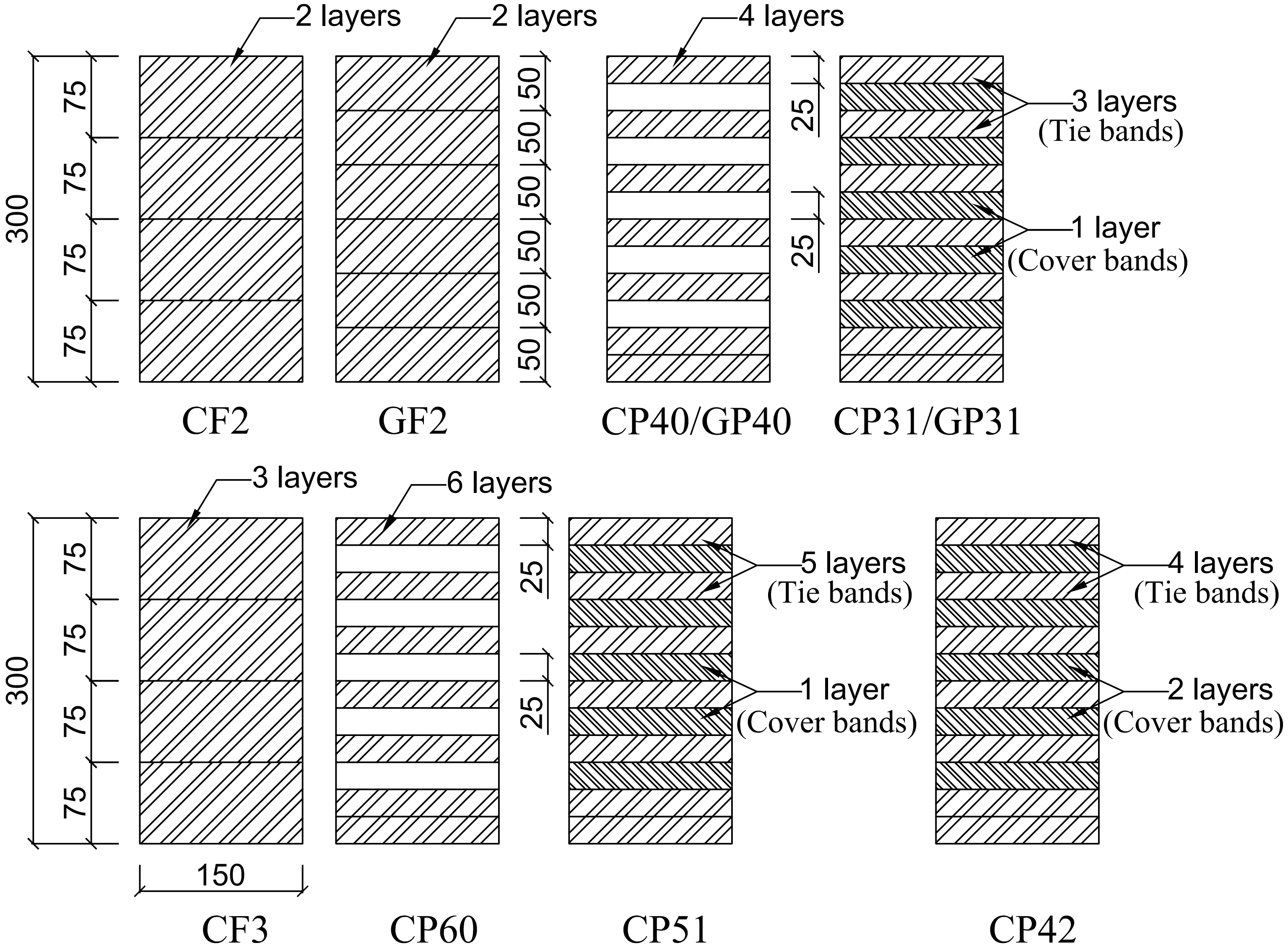
2 layers
2 layers
4 layers
300
75
75
75
75
50
50
50
50
50
50
25
25
3 layers
(Tie bands)
1 layer
(Cover bands)
CF2
GF2
CP40/GP40
CP31/GP31
3 layers
6 layers
300
75
75
75
75
25
25
5 layers
(Tie bands)
1 layer
(Cover bands)
4 layers
(Tie bands)
2 layers
(Cover bands)
150
CF3
CP60
CP51
CP42

Fig. 3

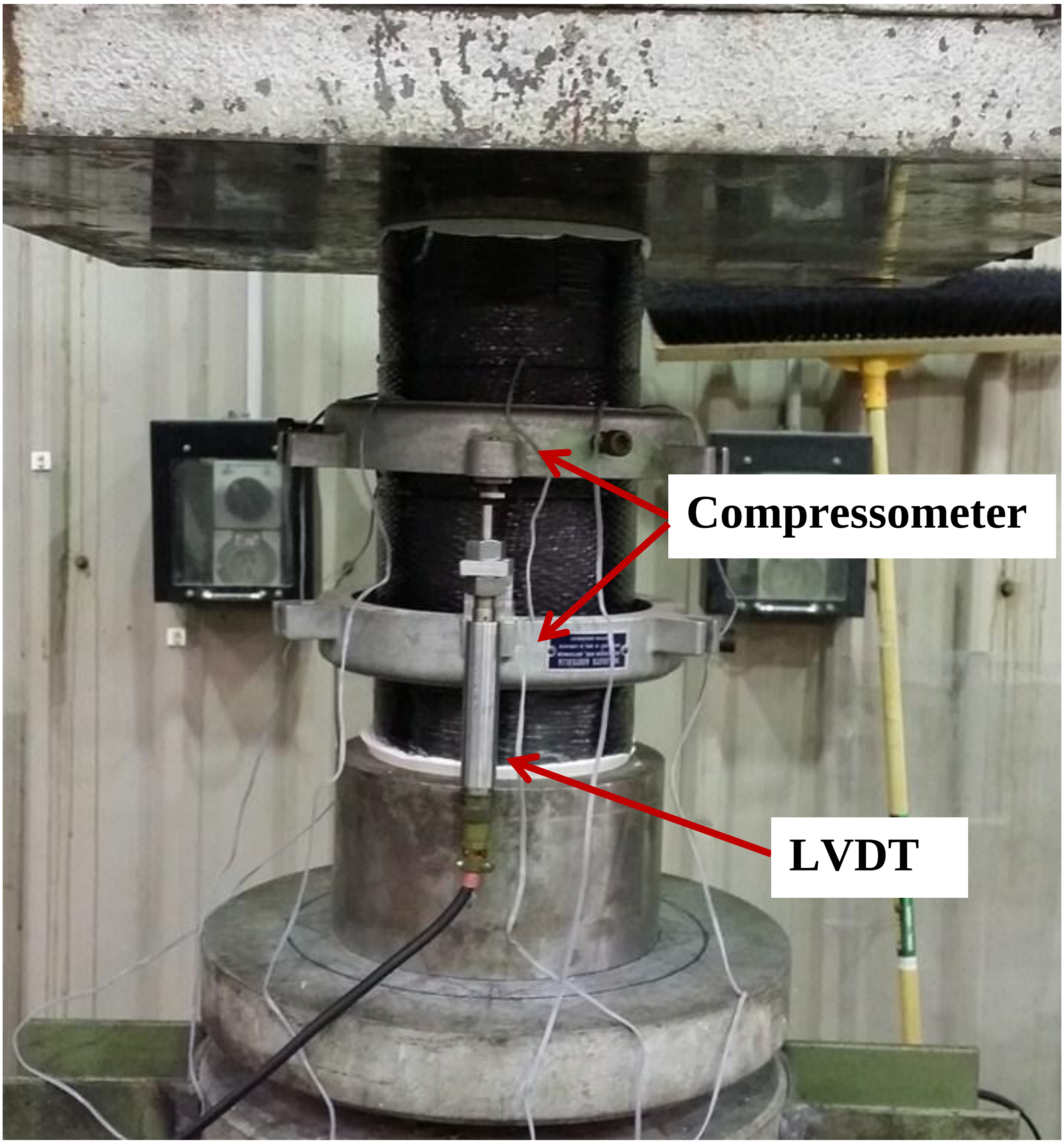

Fig. 4

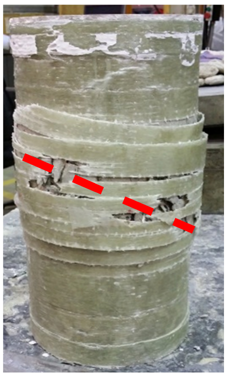

4a. GF2

4b. CP40 ($\sigma_c = f_{co}'$)

4c. CP40 ($\sigma_c \sim f_{cu}'$)

4d. CP60

4e. GP40

4f. GP31

Fig. 5

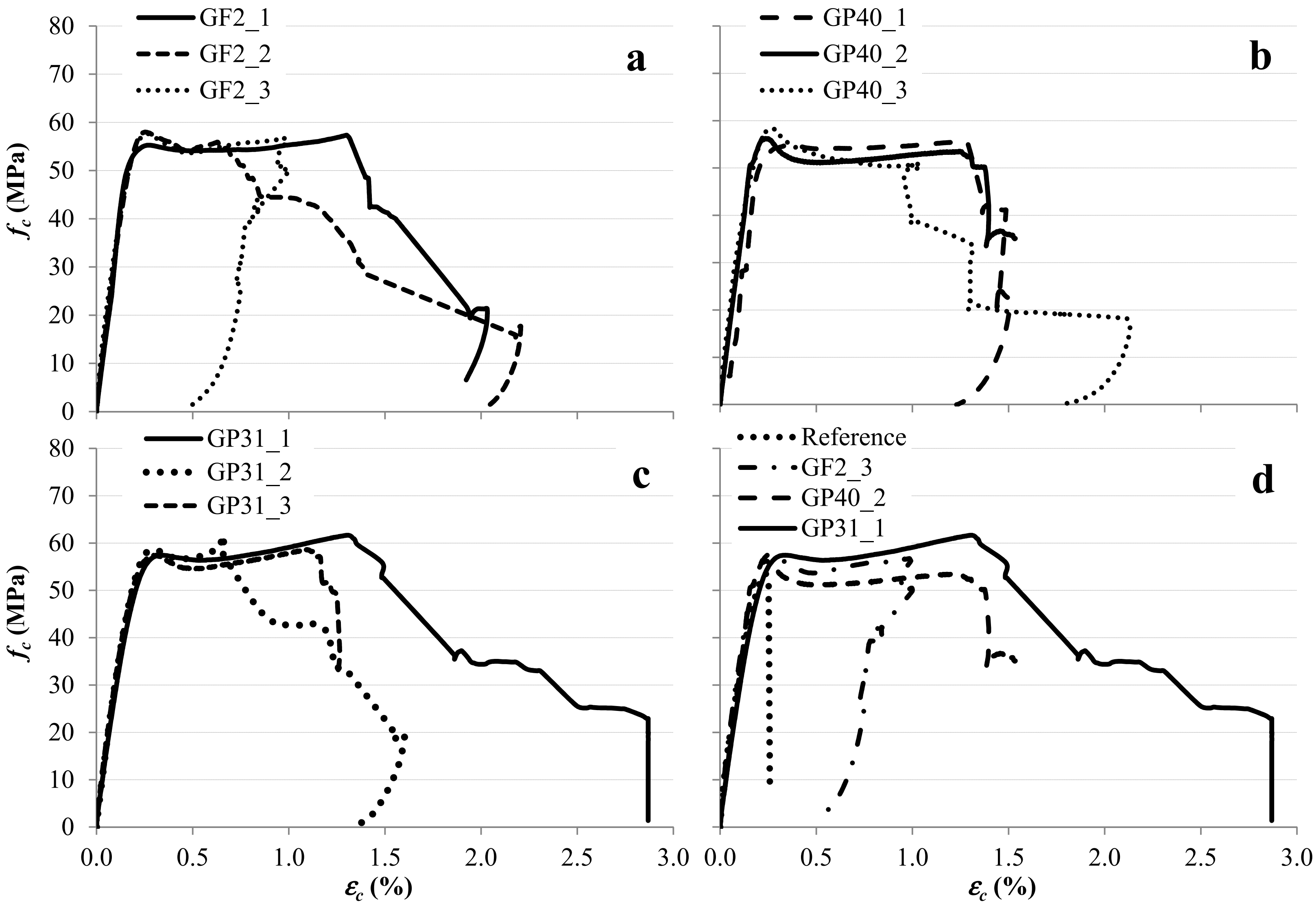

GF2_1
GF2_2
GF2_3
a
GP40_1
GP40_2
GP40_3
b
GP31_1
GP31_2
GP31_3
c
Reference
GF2_3
GP40_2
GP31_1
d
f_c (MPa)
ε_c (%)
0
10
20
30
40
50
60
70
80
0.0
0.5
1.0
1.5
2.0
2.5
3.0

Fig. 6

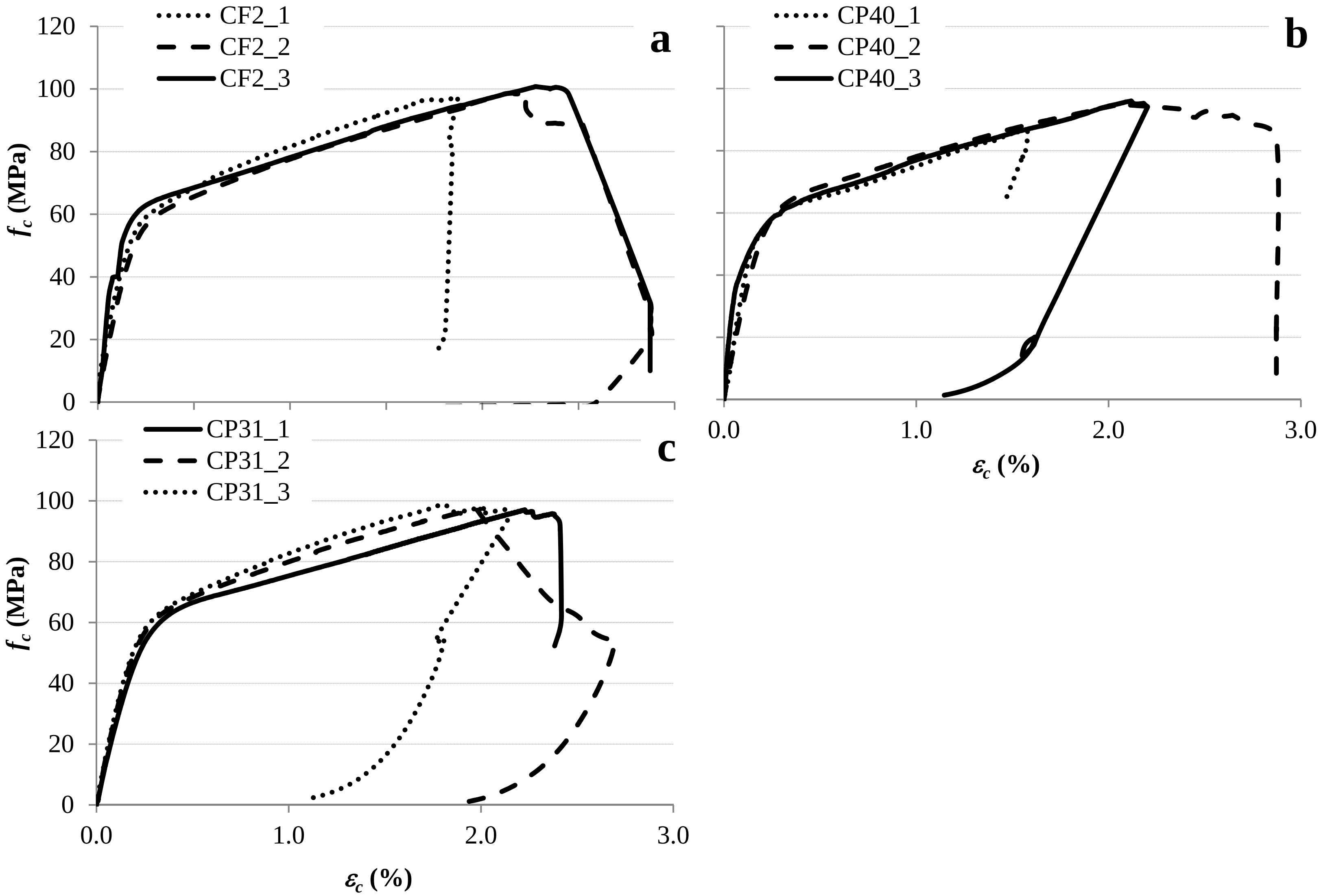

CF2_1
CF2_2
CF2_3
a
CP40_1
CP40_2
CP40_3
b
CP31_1
CP31_2
CP31_3
c
f_c (MPa)
ε_c (%)
0
20
40
60
80
100
120
0.0
1.0
2.0
3.0

Fig. 7

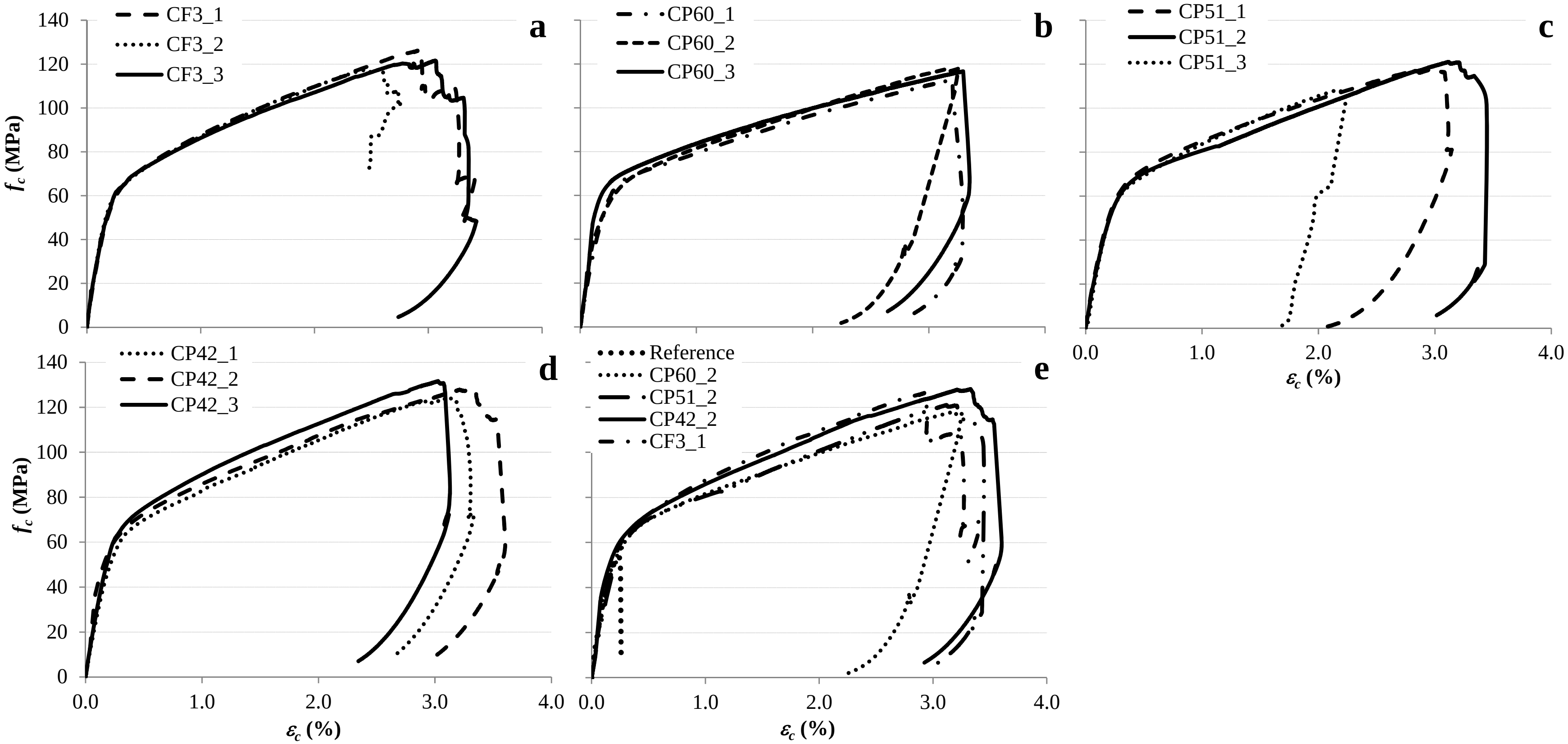

a
CF3_1
CF3_2
CF3_3
b
CP60_1
CP60_2
CP60_3
c
CP51_1
CP51_2
CP51_3
d
CP42_1
CP42_2
CP42_3
e
Reference
CP60_2
CP51_2
CP42_2
CF3_1
f_c (MPa)
ε_c (%)
0
20
40
60
80
100
120
140
0.0
1.0
2.0
3.0
4.0

Fig. 8

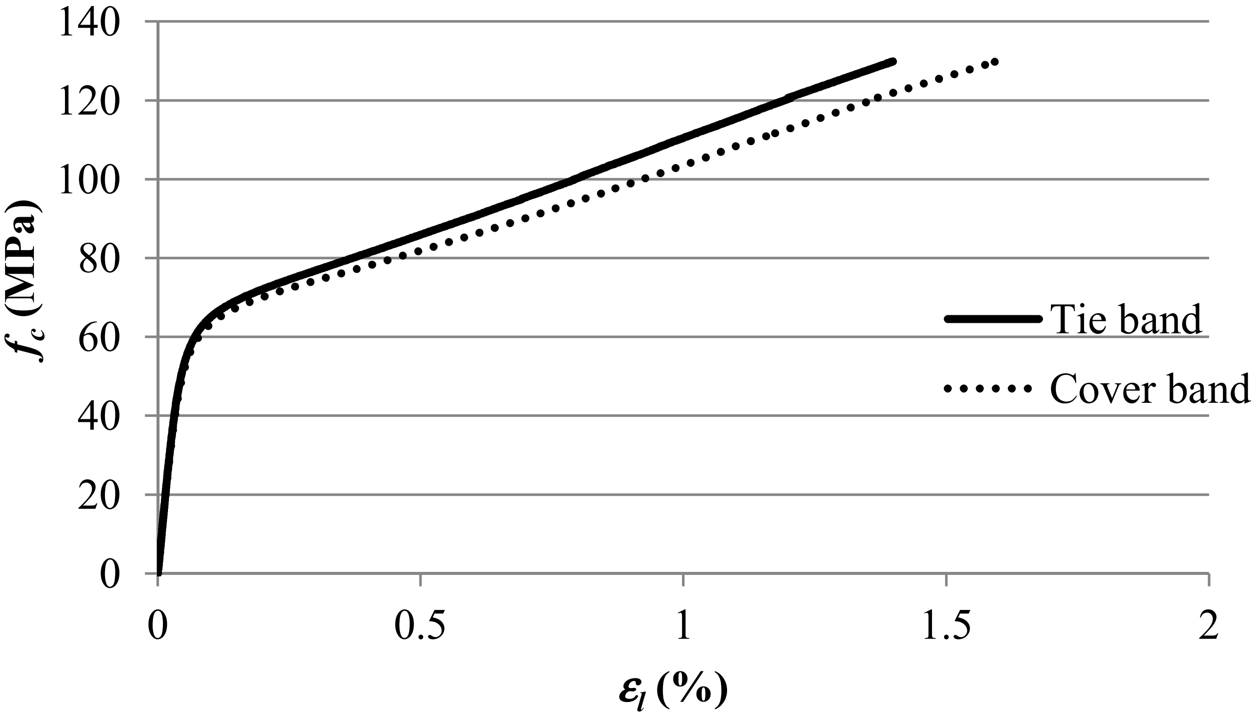

140
120
100
80
60
40
20
0
0
0.5
1
1.5
2
f_c (MPa)
ε_l (%)
Tie band
Cover band